Irreversible bimolecular chemical reactions on directed scale-free networks

Sungchul Kwon* and Yup Kim†

Department of Physics and Research Institute of Basic Sciences, Kyung Hee University, Seoul 130-701, Korea

(Received 27 May 2013; revised manuscript received 16 September 2013; published 30 October 2013)

Kinetics of irreversible bimolecular chemical reactions $A + A \to 0$ and $A + B \to 0$ on directed scale-free networks with the in-degree distribution $P_{\rm in}(k) \sim k^{-\gamma_{\rm in}}$ and the out-degree distribution $P_{\rm out}(\ell) \sim \ell^{-\gamma_{\rm out}}$ are investigated. Since the correlation between k and ℓ of each node generally exists in directed networks, we control the correlation $\langle k\ell\rangle$ with the probability $r \in [0,1]$ by two different algorithms for the construction of the directed networks, i.e., the so-called k and ℓ algorithms. For $r = 1$, the k algorithm gives $\langle k\ell\rangle = \langle k^2\rangle$, whereas the ℓ algorithm gives $\langle k\ell\rangle = \langle \ell^2\rangle$. For $r = 0$, $\langle k\ell\rangle = \langle k\rangle\langle \ell\rangle$ for both algorithms. The kinetics of both reactions are analyzed using heterogeneous mean-field (HMF) theory and Monte Carlo simulations. The density of particles (ρ) algebraically decays in time t as $\rho(t) \sim t^{-\alpha}$. The kinetics of both reactions are determined by the same rate equation, $d\rho/dt = a\rho^2 + b\rho^{\theta-1}$, apart from coefficients. The exponent θ is determined by the algorithm: $\theta = \gamma_{\rm in}$ for the k algorithm ($r \geqslant 0$) and $\theta = \gamma_{\rm min}$ for the ℓ algorithm ($r > 0$), where $\gamma_{\rm min}$ is the smaller exponent between $\gamma_{\rm in}$ and $\gamma_{\rm out}$. For $\theta > 3$, one observes the ordinary mean-field kinetics, $\rho \sim 1/t$ ($\alpha = 1$). In contrast, for $\theta < 3$, $\rho(t)$ anomalously decays with $\alpha = 1/(\theta - 2)$. The HMF predictions are confirmed by the simulations on quenched directed networks.

DOI: 10.1103/PhysRevE.88.042148 PACS number(s): 05.70.Ln, 89.75.Hc, 89.75.Da

I. INTRODUCTION

The bimolecular reactions $A + A \to 0$ and $A + B \to 0$ have been extensively studied because of wide applications to various fields such as physics, chemistry, and biology [1–14]. In both reactions, when two reactants encounter each other on the same site, the reaction takes places instantaneously and both reactants disappear from the system. To understand the properties of the reactions, reaction-diffusion processes have been studied extensively on regular lattices [5–8]. Moreover, the reaction-diffusion processes on complex networks have also been studied because of the anomalous behavior that is distinct from the standard mean-field one on regular lattices [14]. Complex networks exhibit various important structural properties, such as small world, as well as heterogeneous and scale-free degree distributions [15,16], which lead to the anomalous collective phenomena by interplay with the dynamics evolving on networks. In this context, both chemical reactions have been constantly studied on undirected scale-free (SF) networks with the degree distribution $P(q) \sim q^{-\gamma}$ [17–22].

For both reactions, the density of particles (ρ) algebraically decays in time t as $\rho \sim t^{-\alpha}$. For the reactions on d-dimensional regular lattices, there exists the upper critical dimension (d_c). When $d < d_c$, fluctuations in the distributions of particles dominate the kinetics and lead to anomalous decay exponent α ; $\alpha = d/2$ for $A + A \to 0$ [5] and $\alpha = d/4$ for $A + B \to 0$ [6–8]. The anomalous kinetics results from the anticorrelation of reactants for $A + A \to 0$ [5] and the random fluctuations in the initial particle distributions of each species [6–8]. For $d \geqslant d_c$, the uniform mixing of reactants leads to the classical mean-field kinetics with $\alpha = 1$.

On the other hand, unlike on regular lattices, both reactions exhibit the same kinetics because of the uniform mixing of reactants on undirected SF networks [17]. From the systematic mean-field analysis for both reactions [20,21], it was shown that $\rho(t)$ decays as $t^{-\alpha}$ with $\alpha = 1$ for $\gamma > 3$ and $\alpha = 1/(\gamma - 2)$ for $2 < \gamma < 3$. For $\gamma > 3$, the fluctuation in the degree distribution is finite and thus reactions uniformly occur on all nodes to exhibit the same classical mean-field kinetics as on regular lattices with $d \geqslant d_c$. In contrast, for $\gamma < 3$, most reactions occur on hub nodes with a finite fraction of total degree of the network and thus the reaction rate is proportional to the number of hub nodes [20]. As a result, the strong inhomogeneity of the degree distribution of the networks drastically changes the kinetics of both reactions, unlike on regular lattices.

Networks can be classified into undirected and directed ones [14–16]. Many real networks are directed, for instance, the World Wide Web (WWW) [23], email networks [24], neural networks and transcriptional regulation networks [25], and trade networks of livestock [26]. In directed networks, a node receives information via incoming links and sends it via outgoing ones. The effects of the directionality of links on collective behaviors have been studied for various systems such as percolation [27], the voter model [28], the Ising model [29], and epidemic-spreading models [30–32]. It turned out that the directionality plays an important role and leads to nontrivial results that are distinct from those on undirected networks. However, despite the natural occurrence of directed networks and the profound effects of directionality on collective phenomena, reaction-diffusion processes have been mainly studied on undirected networks so far. Hence it is desirous to study various reaction-diffusion processes on directed networks for the comprehensive understanding of the effects of the directionality.

In this paper, the kinetics of the bimolecular reactions on directed SF networks are investigated using heterogeneous mean-field (HMF) theory and Monte Carlo simulations. Directed SF networks are characterized by power-law distributions of in- and out-degrees, $P_{\rm in}(k) \sim k^{-\gamma_{\rm in}}$ and $P_{\rm out}(\ell) \sim \ell^{-\gamma_{\rm out}}$, where k and ℓ denote in-degree and out-degree,

*Present address: Department of Physics, Soongsil University, Seoul 156-743, Korea.

†Corresponding author: ykim@khu.ac.kr

respectively. Since k and ℓ of a node are usually correlated, as in the WWW [23], it is necessary to take into account the correlation between k and ℓ of each node. However, it is *a priori* unknown how the correlation is built up for a given network. In this paper, the correlation $\langle kl\rangle$ of a node is implemented by two different algorithms, i.e., the so-called k and ℓ algorithms. In the k algorithm, k of each node is first assigned by the distribution $P_{\rm in}(k)$. Then, ℓ of each node is set as $\ell = k$ with the probability r or is assigned by the distribution $P_{\rm out}(\ell)$ with $1-r$. In the ℓ algorithm, ℓ of each node is first assigned by the distribution $P_{\rm out}(\ell)$ and then k of each node is set as $k = \ell$ with r or is assigned by the distribution $P_{\rm in}(k)$ with $1-r$. For $r = 1$, the k algorithm gives $\langle kl\rangle = \langle k^2\rangle$, while $\langle kl\rangle = \langle \ell^2\rangle$ is given for the ℓ algorithm. For $r = 0$, $\langle kl\rangle = \langle k\rangle\langle \ell\rangle$ for both algorithms.

We now briefly summarize the results of the HMF theory. The HMF theory predicts the same kinetics for both reactions. $\rho(t)$ decays as $t^{-\alpha}$, but α depends on the algorithm. For the k algorithm and the uncorrelated cases ($r = 0$) of both algorithms, the HMF theory predicts $\alpha = 1/(\gamma_{\rm in}-2)$ for $\gamma_{\rm in} < 3$ and $\alpha = 1$ for $\gamma_{\rm in} > 3$ regardless of $\gamma_{\rm out}$. Since particles flow into a node through the incoming links of the node, the particle density of a node is proportional to the in-degree. As a result, the kinetics is determined by $P_{\rm in}(k)$, which leads to $\gamma_{\rm in}$-dependent α. On the other hand, for the ℓ algorithm, $P_{\rm in}(k)$ is modified by $P_{\rm out}(\ell)$ and thus the particle density on a node depends on the out-degree if $\gamma_{\rm out} < \gamma_{\rm in}$. Therefore, for the ℓ algorithm, the kinetics is affected and determined by the smaller degree exponent $\gamma_{\rm min}$ between $\gamma_{\rm in}$ and $\gamma_{\rm out}$; $\alpha = 1$ for $\gamma_{\rm min} > 3$ and $\alpha = 1/(\gamma_{\rm min}-2)$ for $2 < \gamma_{\rm min} < 3$, respectively. To confirm the predictions of the HMF theory, Monte Carlo simulations are performed on the quenched directed SF networks.

This paper is organized as follows. The HMF analyses are given in Sec. II. Results of Monte Carlo simulations for both reactions are explained in Sec. III. Finally, the summary and relevant discussions are given in Sec. IV.

II. HETEROGENEOUS MEAN-FIELD ANALYSIS

The kinetics of the reactions on directed SF networks with $P_{\rm in} = A_{\rm in}k^{-\gamma_{\rm in}}$ and $P_{\rm out} = A_{\rm out}\ell^{-\gamma_{\rm out}}$ are analyzed by the HMF theory. From now on, a node with in-degree k and out-degree ℓ is denoted as (k,ℓ).

The reaction $A + A \to 0$ on the networks is defined as follows. A node (k_i,ℓ_i) is first selected randomly. If the node is occupied by a particle, one of the ℓ_i outgoing links is randomly selected. Then the particle on (k_i,ℓ_i) moves to the target node (k_j,ℓ_j) connected by the selected outgoing link if (k_j,ℓ_j) is empty. If (k_j,ℓ_j) is occupied by another A particle, the reaction occurs instantaneously and the particles on the two nodes annihilate.

The reaction $A + B \to 0$ is similarly defined by considering the hard-core interaction between like particles. Hence, if the target node is occupied by a like particle, then the hopping attempt is rejected. If an unlike particle occupies the target node, then the reaction occurs.

A. The HMF analysis for $A + A \to 0$

The HMF analysis for $A + A \to 0$ is first presented. For the analysis, we consider the density $\rho_{k\ell}$ of particles averaged over the set of nodes with the same degree k and ℓ. Then, $\rho_{k\ell}$ for $A + A \to 0$ satisfies the rate equation

$$d\rho_{k\ell}/dt = -\rho_{k\ell} + k(1-2\rho_{k\ell})\Theta. \tag{1}$$

The first term represents the outflow of a particle from a node (k,ℓ). The second term consists of the inflow of a particle into an empty node (k,ℓ) and the reaction of a particle on a node (k,ℓ) with an incoming particle. Hence, Θ is the current of particles into node (k,ℓ) defined as $\Theta = \sum_{k',\ell'} \rho_{k'\ell'}T(k\ell;k'\ell')P(k,\ell|k',\ell')$. Here, $T(k\ell;k'\ell')$ is the hopping probability from a node (k',ℓ') to (k,ℓ), and $P(k,\ell|k',\ell')$ is the conditional probability that (k,ℓ) is connected by an outgoing link of (k',ℓ').

For the uncorrelated networks without the degree-degree correlation between any pair of nodes, $P(k',\ell'|k,\ell)$ is given by $P(k,\ell|k',\ell') = \ell' P(k',\ell')/\langle\ell\rangle$ [32]. $P(k,\ell)$ is the joint probability of a node having in-degree k and out-degree ℓ. For the random hopping on the uncorrelated networks, $T(k\ell;k'\ell') = 1/\ell'$, $\Theta = \rho/\langle\ell\rangle$ and one obtains

$$d\rho_{k\ell}/dt = -\rho_{k\ell} + \frac{k(1-2\rho_{k\ell})}{\langle\ell\rangle}\rho, \tag{2}$$

where ρ is the total density with $\rho = \sum_{k,\ell}\rho_{k\ell}P(k,\ell)$. The rate equation of $\rho(t)$ for the directed networks with $\langle k\rangle = \langle\ell\rangle$ becomes

$$d\rho/dt = -2\rho\langle k\rho_{k\ell}\rangle/\langle\ell\rangle. \tag{3}$$

Since $\rho(t)$ algebraically decays in time, $d\rho/dt$ in Eq. (3) decays rapidly in time and thus $d\rho/dt \to 0$ in the long-time limit. Using a quasistatic approximation which sets $d\rho/dt = 0$ and $d\rho_{k\ell}/dt = 0$ [20], one obtains, from Eq. (2) in the long-time limit,

$$\rho_{k\ell} = \frac{k\rho/\langle\ell\rangle}{1+2k\rho/\langle\ell\rangle} = \frac{k/k_c}{2(1+k/k_c)}, \tag{4}$$

where k_c is a crossover degree defined as $k_c \equiv \langle\ell\rangle/2\rho$ and diverges in the limit $\rho \to 0$. $\rho_{k\ell}$ depends only on k and scales with k as $\rho_{k\ell} = 1/2$ for $k \gg k_c$ and $\rho_{k\ell} \sim k$ for $k \ll k_c$, as on undirected SF networks [20,22]. Thus, $d\rho/dt$ in Eq. (3) is determined by the term $\langle k\rho_{k\ell}\rangle/\langle\ell\rangle$ written as

$$\frac{\langle k\rho_{k\ell}\rangle}{\langle\ell\rangle} = \frac{1}{4\rho}\int_1^\infty dk\int_1^\infty d\ell\,\frac{(k/k_c)^2P(k,\ell)}{1+k/k_c}. \tag{5}$$

Since $P(k,\ell)$ depends on the correlation $\langle k\ell\rangle$, Eq. (3) depends on the algorithm employed to construct the directed networks.

1. The k algorithm

In the k algorithm, the out-degree ℓ of a node with the preassigned in-degree k is set as $\ell = k$ with a probability $r \in [0,1]$. Thus, the conditional probability $P(\ell|k)$ of a node with k having ℓ is $P(\ell|k) = r\delta_{k\ell} + (1-r)P_{\rm out}(\ell)$. With $P(k,\ell) = P(\ell|k)P_{\rm in}(k)$, one obtains the joint probability $P(k,\ell)$ for the k algorithm as

$$P(k,\ell) = r\delta_{k\ell}P_{\rm in}(k) + (1-r)P_{\rm in}(k)P_{\rm out}(\ell). \tag{6}$$

Then, Eq. (5) becomes

$$\frac{4\rho\langle k\rho_{k\ell}\rangle}{\langle\ell\rangle} = \int_1^\infty dk \frac{(k/k_c)^2 P_{\rm in}(k)}{1+k/k_c}. \tag{7}$$

Interestingly, the integral in Eq. (7) is independent of the correlation r and out-degree. Since $\rho_{k\ell}$ depends on only in-degree, $\langle k\rho_{k\ell}\rangle$ is independent of $P_{\rm out}(\ell)$. Hence, there are no effects of the correlation on the rate equation. Therefore, Eq. (7) also holds for the uncorrelated case ($r = 0$) of both algorithms.

Integrating Eq. (7) with $P_{\rm in}(k) = A_{\rm in}k^{-\gamma_{\rm in}}$ [32], one obtains $d\rho/dt$ from Eq. (3) in the limit $t \to \infty$,

$$\frac{d\rho}{dt} = -a\rho^2 - d_{\rm in}\rho^{\gamma_{\rm in}-1}. \tag{8}$$

Here, a and $d_{\rm in}$ are nondiverging coefficients. Therefore, $\rho(t)$ decays as $t^{-\alpha}$ with $\alpha = 1/(\gamma_{\rm in}-2)$ for $\gamma_{\rm in} < 3$ and $\alpha = 1$ for $\gamma_{\rm in} > 3$. This result is independent of r and the kinetics is the same as that on the undirected SF networks with the degree distribution $P(q) \sim q^{-\gamma}$ [20], except that $\gamma_{\rm in}$ replaces γ.

2. *The ℓ algorithm*

In the ℓ algorithm, the in-degree k of a node with the preassigned out-degree ℓ is set as $k = \ell$ with the probability r. Then the conditional probability $P(k|\ell)$ of a node with ℓ having k is $P(k|\ell) = r\delta_{k\ell} + (1-r)P_{\rm in}(k)$. With $P(k,\ell) = P(k|\ell)P_{\rm out}(\ell)$, one obtains $P(k,\ell)$ for the ℓ algorithm as

$$P(k,\ell) = r\delta_{k\ell}P_{\rm out}(\ell) + (1-r)P_{\rm in}(k)P_{\rm out}(\ell). \tag{9}$$

With the same method used in the k algorithm, $d\rho/dt$ for the ℓ algorithm is written as

$$d\rho/dt = -b\rho^2 - rd_{\rm out}\rho^{\gamma_{\rm out}-1} - (1-r)d_{\rm in}\rho^{\gamma_{\rm in}-1}. \tag{10}$$

Here, b and $d_{\rm out}$ are also nondiverging coefficients, and $d_{\rm in}$ is exactly the same coefficient in Eq. (8). As expected, $P_{\rm out}(\ell)$ affects the kinetics and, as a result, the r-dependent second term appears in the final rate equation. Since the last two terms in Eq. (10) compete with each other, the term with the smaller degree exponent dominates the kinetics. Therefore, $d\rho/dt$ can be written in a simple form as

$$d\rho/dt = -a\rho^2 - d_{\rm min}\rho^{\gamma_{\rm min}-1}, \tag{11}$$

where $\gamma_{\rm min}$ is the smaller exponent between $\gamma_{\rm in}$ and $\gamma_{\rm out}$, and $d_{\rm min}$ is the coefficient of the term with $\gamma_{\rm min}$ in Eq. (11). Then, for $r > 0$, one obtains $\alpha = 1/(\gamma_{\rm min}-2)$ for $\gamma_{\rm min} < 3$ and $\alpha = 1$ for $\gamma_{\rm min} > 3$.

B. The HMF analysis of $A + B \to 0$

For $A + B \to 0$, the hard-core repulsion between like particles is considered. The reaction proceeds from initial configurations with the same density of A and B particles, $\rho^A(0) = \rho^B(0)$. Initially, particles are randomly distributed over nodes without multiple occupation. The equality $\rho^A(t) = \rho^B(t)$ is then maintained at any time.

The density $\rho^A_{k\ell}$ is also defined as the density of A particles averaged over the set of nodes with the same degree k and ℓ. For the uncorrelated directed networks, $d\rho^A_{k\ell}/dt$ is written as

$$\frac{d\rho^A_{k\ell}}{dt} = -\rho^A_{k\ell} + \frac{k}{\langle\ell\rangle}\sum_{k',\ell'}\left[(1-\rho_{k\ell})\rho^A_{k'\ell'} - \rho^A_{k\ell}\rho^B_{k'\ell'}\right]P(k',\ell'). \tag{12}$$

With $\rho_{k\ell} = \rho^A_{k\ell} + \rho^B_{k\ell} = 2\rho^A_{k\ell}$ and $\rho^A = \sum_{k,\ell}\rho^A_{k\ell}P(k,\ell)$, Eq. (12) is written as

$$d\rho^A_{k\ell}/dt = -\rho^A_{k\ell} + \frac{k\left(1-3\rho^A_{k\ell}\right)}{\langle\ell\rangle}\rho^A. \tag{13}$$

Then, using the quasistatic approximation, one obtains

$$\rho^A_{k\ell} = \frac{k\rho^A/\langle\ell\rangle}{1+3k\rho^A/\langle\ell\rangle} = \frac{k/k_c}{3(1+k/k_c)}, \tag{14}$$

where $k_c = \langle\ell\rangle/3\rho^A$. $(d\rho^A/dt)$ is thus given as

$$d\rho^A/dt = -3\rho^A\langle k\rho^A_{k\ell}\rangle/\langle\ell\rangle. \tag{15}$$

Compared with $d\rho_{k\ell}/dt$ for $A + A \to 0$ in Eq. (2), the difference in Eq. (13) is only the numerical prefactor "3." Therefore, the time dependence of densities is identical in both reactions. As a result, the kinetics of $A + B \to 0$ is the same as that of $A + A \to 0$ for both algorithms.

On the directed networks, the reactions and the inflow of particles into a node are controlled by the in-degree distribution. As a result, the kinetics on the directed SF networks are determined by the in-degree distribution. In contrast, the out-degree distribution only comes into play in the case where the in-degree distribution is modified by the out-degree distribution, as in the ℓ algorithm. In that case, the kinetics is modified only for $\gamma_{\rm out} < \gamma_{\rm in}$.

For both algorithms, the decay exponent α is given by the same equation as that on the undirected networks. It implies that the mechanism for the anomalous kinetics is nearly identical for both undirected and directed SF networks. The reactants are uniformly mixed in networks, which wipes out the depletion zone by the anticorrelation for $A + A \to 0$ and the segregation of unlike particles for $A + B \to 0$ [17–22].

In the directed networks, particles move toward the hub nodes with a large fraction of incoming links and thus most reactions occur on the hub nodes. In particular, hub nodes with in-degree $k \gg k_c$ are the drains of particles through which particles disappear due to the reactions. As a result, the reaction rate is proportional to the number of hub nodes with $k \gg k_c$, as in undirected SF networks [20]. Therefore, one can heuristically obtain $d\rho/dt$ for both reactions as follows. $d\rho/dt$ is given as $d\rho/dt \sim -\int_1^\infty d\ell \int_{k_c}^\infty dk P(k,\ell)$, where $k_c \sim 1/\rho$ for both reactions. From Eqs. (6) and (9), one obtains $d\rho/dt \sim -k_c^{1-\gamma_{\rm in}}$ for the k algorithm and $d\rho/dt \sim -rk_c^{1-\gamma_{\rm out}} - (1-r)k_c^{1-\gamma_{\rm in}}$ for the ℓ algorithm, respectively, which give the same kinetics as those predicted by the HMF theory for both reactions.

III. MONTE CARLO SIMULATIONS

To confirm the predictions of the HMF theory, Monte Carlo simulations of both reactions are performed on quenched directed SF networks. The networks of size N with

$P_{\rm in}(k) = A_{\rm in}k^{-\gamma_{\rm in}}$ and $P_{\rm out}(\ell) = A_{\rm out}\ell^{-\gamma_{\rm out}}$ are first constructed by taking the following steps.

(i) First, the in-degree k and the out-degree ℓ of each node are assigned by the following algorithm [32,33]. The number N_k of nodes with k is deterministically calculated from $N_k = {\rm int}[N\sum_{k'\geqslant k} P_{\rm in}(k')] - {\rm int}[N\sum_{k'\geqslant(k+1)} P_{\rm in}(k')]$ for $k \in [k_{\rm min},k_{\rm max}]$, where int$[x]$ denotes the integer part of a real variable x [33]. We set $k_{\rm min} = 2$, $k_{\rm max} = N^{1/(\gamma_{\rm in}-1)}$. Then, to assign the in-degree k to N_k nodes, N_k nodes are randomly selected among nodes which are not yet assigned in-degree. By repeating this step from $k_{\rm max}$ to $k_{\rm min}$, the in-degree sequence $\{k_1,\ldots,k_N\}$ for the N nodes is generated. With the same method for $\ell \in [2,N^{1/(\gamma_{\rm out}-1)}]$, the out-degree sequence $\{\ell_1,\ldots,\ell_N\}$ is generated.

(ii) For the correlation between the in-degree and out-degree of each node, the generated degree sequences are modified in the following way. In the k algorithm, the generated in-degree sequence $\{k_1,\ldots,k_N\}$ is used without modification. Then, the out-degree ℓ_i of a node i having in-degree k_i is set as $\ell_i = k_i$ with probability r or one can leave ℓ_i as it is in the generated out-degree sequence with probability $(1-r)$. In the ℓ algorithm, the processes are reversed. The generated out-degree sequence $\{\ell_1,\ldots,\ell_N\}$ is used without modification. Then, the in-degree of a node is modified in the similar way as in the k algorithm.

(iii) In the directed network, the total in-degree $K = \sum_{i=1}^{N} k_i$ should be equal to the total out-degree $L = \sum_{1}^{N} \ell_i$ because an incoming link of a node is an outgoing link of another. If the generated sequences in step (ii) do not satisfy the constraint $K = L$, the sequences are modified in the following way. In the k algorithm, one of the nodes whose out-degrees are not changed in step (ii) is randomly chosen. Then, the out-degree of the chosen node is replaced with a new one randomly chosen from the unmodified out-degree sequence in step (i). In this process, the correlation built in step (ii) is preserved. If the new out-degree reduces the difference $|K-L|$, then the new out-degree replaces the old one. This step is repeated until $K = L$ holds.

(iv) Finally, the network is constructed by connecting nodes with directed links. Each directed link is made by matching an outgoing link of a node to an incoming link of another node. For the connection of all nodes, an uncorrelated configuration model (method) (UCM) [34] is used. In the UCM, two lists are created. One is the K list of size $K = \sum_i k_i$ and the other is the L list of size $L = \sum_i \ell_i$. A node i with k_i and ℓ_i is recorded k_i times in the K list and ℓ_i times in the L list. In this way, all nodes are recorded in each list. Then, for the connection of a pair of nodes, one element is randomly selected in each list. If the two selected elements are identical or have already been connected by a directed link, then the pair is discarded. Otherwise, a directed link between the selected pair is created. After the creation of the new link, each element of the selected pair is removed from each list. This step is repeated until all elements are eliminated from the two lists.

By taking steps (i)–(iv), it is confirmed for the SF networks with $N \leqslant 10^7$ that the networks are constructed without any fragmentation and there exists at least one directed path between any pair of nodes. On these quenched directed SF networks, we perform simulations for both reactions.

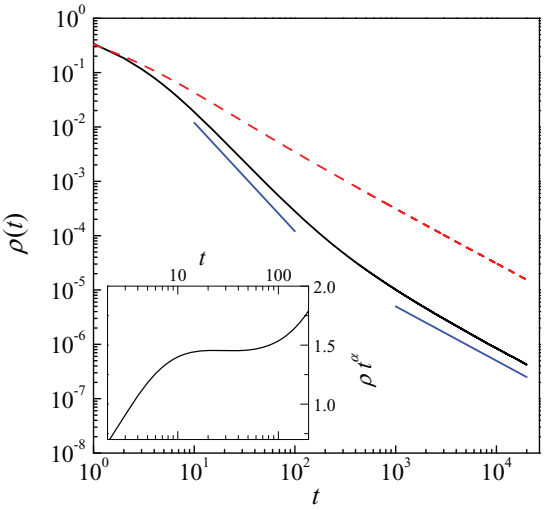

FIG. 1. (Color online) Simulation results of $A + A \to 0$ for the k algorithm with $r = 0$. The main plot shows $\rho(t)$ for $(\gamma_{\rm in},\gamma_{\rm out}) = (3.5,4.0)$ (dashed curve) and for (2.5,3.5) (solid curve). The solid lines represent the HMF theory with $\alpha_{\rm HMF} = 2$ for $\gamma_{\rm in} = 2.5$ and the decay with $\alpha = 1$. The inset shows the scaling plot of ρt^{α} against t with $\alpha = 1.87$ for (2.5,3.5).

A. $A + A \to 0$

Simulation results of $A + A \to 0$ for each algorithm are first presented. For the network average, 100 different networks of size $N = 10^7$ are used for both algorithms.

For the k algorithm, the HMF theory predicts $\rho(t) \sim t^{-\alpha_{\rm HMF}}$ with $\alpha_{\rm HMF} = 1/(\gamma_{\rm in}-2)$ for $\gamma_{\rm in} < 3$, and $\alpha_{\rm HMF} = 1$ otherwise. The kinetics is independent of the correlation r for the k algorithm, and the independence is confirmed by simulations for various r. Therefore, the results for $r = 0$ are mainly presented. Simulation results on the networks of $(\gamma_{\rm in},\gamma_{\rm out}) = (2.5,3.5)$ and (3.5,4.0) are shown in Fig. 1. For the networks, the HMF theory predicts $\alpha_{\rm HMF} = 2$ for $\gamma_{\rm in} = 2.5$ and $\alpha_{\rm HMF} = 1$ for $\gamma_{\rm in} = 3.5$, respectively. For $\gamma_{\rm in} = 3.5$, $\rho(t)$ clearly decay as t^{-1} and confirm $\alpha_{\rm HMF} = 1$. However, as the early time data compared to the solid line representing the HMF theory in the main plot of Fig. 1 show, $\rho(t)$ for $\gamma_{\rm in} = 2.5$ decays with α close to $\alpha_{\rm HMF} = 2$ only in early time. In the long-time limit, $\rho(t)$ decays as t^{-1}, which results from finite-size effects of the networks, as in undirected SF networks [22]. Hence, $\rho(t)$ undergoes the crossover from the decay with $\alpha_{\rm HMF}$ to that with $\alpha = 1$ induced by the finite-size effects. Since the finite-size effect comes into play before $\rho(t)$ exhibits the kinetics with $\alpha_{\rm HMF}$, the estimate of α is inevitably smaller than $\alpha_{\rm HMF}$. To estimate α in early time, the scaling plot of ρt^{α} against t is made as shown in the inset of Fig. 1. We estimate $\alpha = 1.87(2)$, which is close to $\alpha_{\rm HMF} = 2$.

For the ℓ algorithm, one expects $\alpha_{\rm HMF} = 1/(\gamma_{\rm min}-2)$ for $\gamma_{\rm min} < 3$, where $\gamma_{\rm min}$ is the smaller value between $\gamma_{\rm in}$ and $\gamma_{\rm out}$. Simulation results on the networks with $(\gamma_{\rm in},\gamma_{\rm out}) = (2.5,3.5)$ and (3.5,2.5) constructed by the ℓ algorithm with $r = 1/2$ are shown in Fig. 2. The HMF theory predicts $\alpha_{\rm HMF} = 2$, because $\gamma_{\rm min} = 2.5$ for both networks. As shown in Fig. 2,

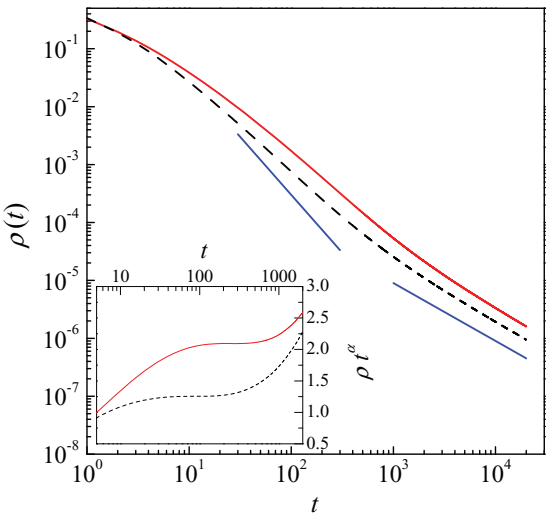

FIG. 2. (Color online) Simulation results of $A + A \to 0$ for the ℓ algorithm with $r = 1/2$. The main plot shows $\rho(t)$ for $(\gamma_{\rm in},\gamma_{\rm out}) = (2.5,3.5)$ (solid curve) and for (3.5,2.5) (dashed curve). The solid lines represent the HMF theory with $\alpha_{\rm HMF} = 2$ for $\gamma_{\rm in} = 2.5$ and the decay with $\alpha = 1$. The inset shows the scaling plot of ρt^{α} vs t with $\alpha = 1.54$ for $\gamma_{\rm in} = 2.5$ and $\alpha = 1.61$ for $\gamma_{\rm in} = 3.5$.

$\rho(t)$ also exhibits the crossover on both networks as for the k algorithm. From the scaling plots, $\alpha = 1.54(2)$ for (2.5,3.5) and $\alpha = 1.61(2)$ for (3.5,2.5) are estimated (see the inset of Fig. 2). The estimate is smaller than $\alpha_{\rm HMF}$ and that for the k algorithm, but it is large enough to confirm the HMF predictions. Figure 3 shows the similar estimates of α from simulations on the networks with various $\gamma_{\rm in}$ and $\gamma_{\rm out} = 3.5$ from both algorithms. The estimates somewhat deviate from the HMF theory, $\alpha_{\rm HMF} = 1/(\gamma_{\rm in} - 2)$ for $\gamma_{\rm in} < 3$ and $\alpha_{\rm HMF} = 1$ for $\gamma_{\rm in} \geqslant 3$, due to the strong finite-size effect, but clearly follow the trend of the HMF theory.

Next, the finite-size effect is discussed. When $\alpha_{\rm HMF} > 1$, the finite-size effects of the networks induce the crossover behavior for both algorithms, as shown in Figs. 1 and 2.

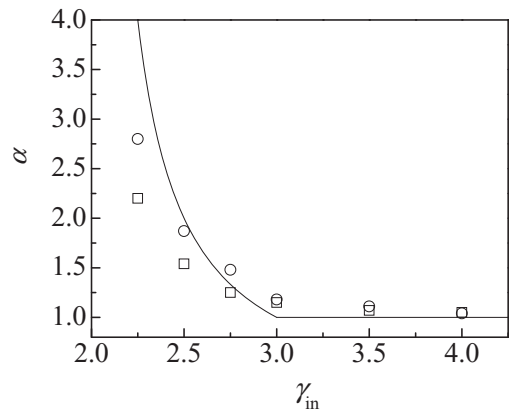

FIG. 3. Plot of α estimated from simulations of $A + A \to 0$ on the networks with varying $\gamma_{\rm in}$ and $\gamma_{\rm out} = 3.5$. Used network size is $N = 10^7$. ○'s denote the estimates for the k algorithm with $r = 0$ and □'s denote those for the ℓ algorithm with $r = 0.5$. The solid curve represents the HMF theory, $\alpha_{\rm HMF} = 1/(\gamma_{\rm in} - 2)$ for $\gamma_{\rm in} < 3$ and $\alpha_{\rm HMF} = 1$ for $\gamma_{\rm in} \geqslant 3$, for both algorithms.

This finite-size effect can be understood from the asymptotic behavior of $\rho_{k\ell}$ in the limit $k_c \to \infty$. For finite-size networks, the maximal in-degree ($k_{\rm max}$) is finite, while $k_c \to \infty$ in the limit $t \to \infty$. Hence, when $k_c > k_{\rm max}$, $\rho_{k\ell} \sim k\rho/\langle k\rangle$ for any k from Eq. (4), which gives $\rho(t) \sim \langle k\rangle t^{-1}/\langle k^2\rangle$ from Eq. (3). Since $\langle k^2\rangle$ does not diverge in finite-size networks, $\rho(t) \sim t^{-1}$ for $k_c > k_{\rm max}$. On the other hand, for $k_c < k_{\rm max}$, the finite-size effect is not activated yet, so $\rho(t)$ tends to follow the HMF theory. Therefore, there exists the crossover time τ_c at which the relation $k_c(\tau_c) = k_{\rm max}$ holds. As a result, $\rho(t)$ tends to follow the HMF theory for $t \ll \tau_c$ and t^{-1} for $t \gg \tau_c$. For the networks with $k_{\rm max} \sim N^{1/(\gamma_{\rm in}-1)}$, τ_c scales with N as [22]

$$\tau_c \sim N^{1/\mu}, \quad \mu = \alpha_{\rm HMF}(\gamma_{\rm in} - 1) \tag{16}$$

because $k_c(\tau_c) \sim 1/\rho(\tau_c)(= \tau_c^{\alpha_{\rm HMF}}) = k_{\rm max}$. The exponent μ depends on the algorithm, i.e., $\mu = (\gamma_{\rm in} - 1)/(\gamma_{\rm in} - 2)$ for the k algorithm ($r \geqslant 0$) and $\mu = (\gamma_{\rm in} - 1)/(\gamma_{\rm min} - 2)$ for the ℓ algorithm, respectively.

To confirm the scaling behavior of Eq. (16), τ_c is numerically measured in the following way [22]. From the simulation data of $\rho(t)$, the time interval in which $\rho(t)$ decays with $\alpha > 1$ is first identified. The time interval in which $\rho(t)$ decays with $\alpha = 1$ is also identified. After identifications, the fitting curve of $\rho(t)$ in each interval is obtained. Then, τ_c is estimated from the intersection of the two fitting curves. $\tau_c(N)$'s for various N up to 10^7 are measured on the networks with $(\gamma_{\rm in},\gamma_{\rm out}) = (2.5,3.5)$ for the k algorithm and on those with (3.5,2.5) for the ℓ algorithm with $r = 1/2$. From the least square fitting of the relation $\tau_c \sim N^{1/\mu}$ to the data in Fig. 4, $1/\mu = 0.33$ for the k algorithm and 0.22 for the ℓ algorithm are obtained. These results agree well with the predictions, i.e., $1/\mu = 1/3$ for the k algorithm and $1/\mu = 1/5$ for the ℓ algorithm.

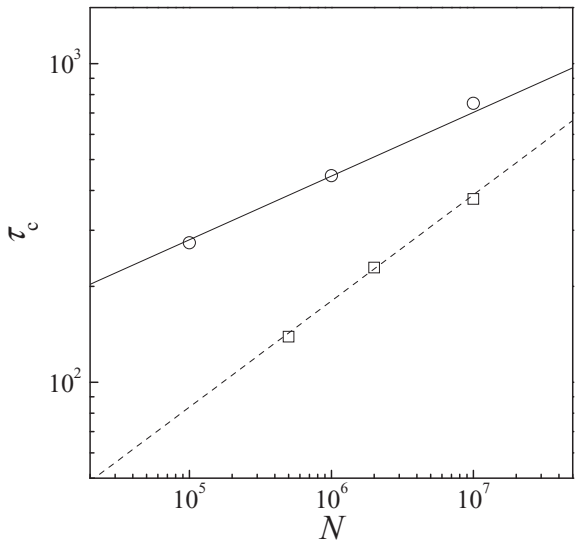

FIG. 4. Plot of $\tau_c(N)$ of $A + A \to 0$ against N. ○'s denote the data for the ℓ algorithm with $r = 1/2$ and □'s denote those for the k algorithm with $r = 0$. $(\gamma_{\rm in},\gamma_{\rm out})$ is set to be (2.5,3.5) for the k algorithm and (3.5,2.5) for the ℓ algorithm, respectively. The lines represent the theoretical results in Eq. (16) with $1/\mu = 1/5$ (solid line) and with $1/\mu = 1/3$ (dashed line), respectively.

As shown in Fig. 4, τ_c is quite small compared with maximal simulation times for even $N = 10^7$ (see Figs. 1 and 2). Hence, in the simulation on the finite-size networks, α should be measured in the shorter initial time interval ($t < \tau_c$). As a result, the estimated α is inevitably underestimated, but is expected to approach to the mean-field value in the limit of $N \to \infty$ or $\tau_c \to \infty$. However, it seems to be practically hard to confirm the HMF exponents because the crossover time very slowly increases with N.

Finally, we examine the validity of the quasistatic approximation employed to obtain Eq. (4) in Sec. II. The important consequence of Eq. (4) is that $\rho_{k\ell}$ depends only on the in-degree k and the existence of the crossover degree $k_c = \langle \ell \rangle / 2\rho$. k_c is not a constant but indefinitely increases in time as $\rho \to 0$. As a result, for $k_c < k_{\max}$, $\rho_{k\ell}$ scales as $\rho_{k\ell} \sim k$ for $k \ll k_c$ and $\rho_{k\ell} = 1/2$ for $k \gg k_c$. For $k_c > k_{\max}$, the finite size affects the kinetics and thus $\rho_{k\ell} \sim k$ for any k. In addition, $\rho_{k\ell}$ is a function of one scaling variable k/k_c. Therefore, Eq. (4) is simply written as

$$\rho_{k\ell} = F(kt^{-\alpha}), \tag{17}$$

where $F(x) = 1/2$ for $x \gg 1$ and $F(x) \simeq x$ for $x \ll 1$. The scaling relation (17) includes most information for the kinetics and also provides another way to measure α for $t < \tau_c$. Hence the validity of the quasistatic approximation and Eq. (4) can be confirmed by examining the scaling relation (17).

To confirm Eq. (17), $\rho_{k\ell}$ should be measured as a function of k and ℓ. However, since $\rho_{k\ell}$ depends only on k, we instead measure ρ_k, the average density of particles on the nodes with the same in-degree k. Figure 5(a) shows ρ_k measured

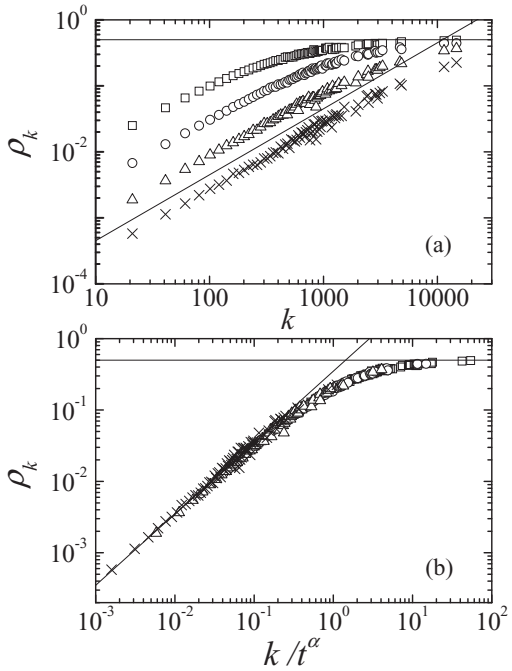

FIG. 5. (a) Plot of $\rho_k(t)$ of $A + A \to 0$ for the k algorithm with $r = 0$ against k at $t = 20\,(\square), 40\,(\circ), 80\,(\triangle)$, and $160\ (\times)$. Used networks are those with $\gamma_{\text{in}} = 2.5$, $\gamma_{\text{out}} = 3.5$ and $N = 10^7$. (b) Scaling plot of ρ_k against $kt^{-\alpha}$ with $\alpha = 1.87$. In (a) and (b), solid lines represent the theoretical relations $\rho_k \sim k$ for $k \ll k_c$ and $\rho_k = 1/2$ for $k \gg k_c$.

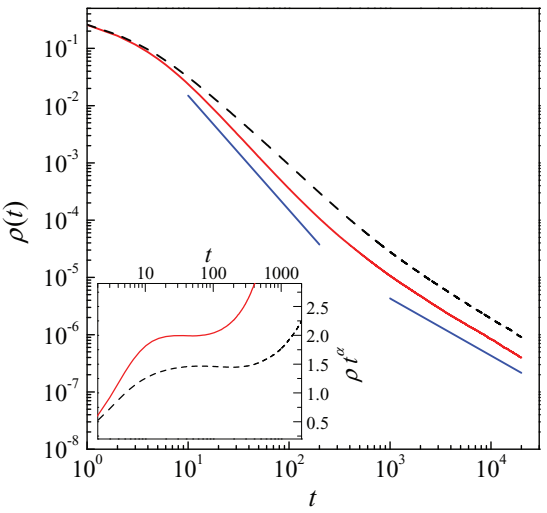

FIG. 6. (Color online) Simulation results of $A + B \to 0$. The solid curve denotes the data on the networks with $(\gamma_{\text{in}}, \gamma_{\text{out}}) = (2.5, 3.5)$ from the k algorithm with $r = 0$ and the dashed curve denotes the data on the networks with (3.5,2.5) from the ℓ algorithm with $r = 1/2$. The solid lines represent the HMF theory with $\alpha_{\text{HMF}} = 2$ and the decay with $\alpha = 1$. The inset shows the scaling plot of $\rho^A t^\alpha$ against t with $\alpha = 1.88$ for the k algorithm and the plot with $\alpha = 1.60$ for the ℓ algorithm.

at various time steps on the networks of $(\gamma_{\text{in}}, \gamma_{\text{out}}) = (2.5, 3.5)$ for the k algorithm with $r = 0$. ρ_k at $t = 160$ linearly increases with k without saturation, which implies $k_c > k_{\max}$. Hence, the finite-size effect already appears at $t = 160$, which agrees with the behavior of ρ in Fig. 1. For $t \leqslant 80$, ρ_k linearly increases for small k and finally saturates to $1/2$ for sufficiently large k, as expected. To confirm the scaling relation (17), ρ_k for various times are plotted against $kt^{-\alpha}$ by varying α. As shown in Fig. 5(b), the best scaling collapse occurs at $\alpha = 1.87$, which coincides with the estimated α obtained from the scaling plot in Fig. 1. Therefore, it is numerically confirmed that the quasistatic approximation is valid and thus Eq. (4) correctly describes the kinetics of $A + A \to 0$.

B. $A + B \to 0$

Simulations for $A + B \to 0$ are carried out on the same networks as those used for simulations for $A + A \to 0$. Initially, A and B particles with the condition $\rho^A(0) = \rho^B(0) = 1/2$ are randomly distributed over the nodes without multiple occupation of like particles on a node. The HMF theory of Eqs. (14) and (15) predicts the same kinetics as that of $A + A \to 0$; $\alpha_{\text{HMF}} = 1/(\gamma_{\text{in}} - 2)$ for the k algorithm and $1/(\gamma_{\min} - 2)$ for the ℓ algorithm.

Figure 6 shows $\rho^A(t)$ on the networks with $(\gamma_{\text{in}}, \gamma_{\text{out}}) = (2.5, 3.5)$ from the k algorithm with $r = 0$ and on the networks of (3.5,2.5) from the ℓ algorithm with $r = 1/2$. The HMF theory predicts $\alpha_{\text{HMF}} = 2$ on the networks of both algorithms. As shown in the main plot of Fig. 6, $\rho^A(t)$ exhibits the crossover from the decay with $\alpha > 1$ in early time to that with $\alpha = 1$ in the long-time limit. From the scaling plot, we estimate $\alpha = 1.88(2)$ for the k algorithm and $\alpha = 1.60(2)$ for the ℓ algorithm (see the inset of Fig. 6), which are also underestimated due to the finite-size effect as in $A + A \to 0$. Figure 7 shows similar

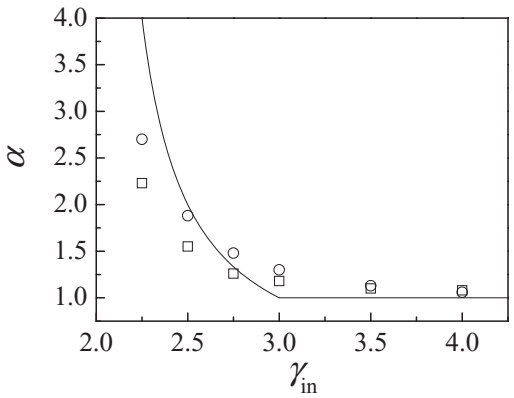

FIG. 7. Plot of α estimated from simulations of $A + B \to 0$ on the networks with varying $\gamma_{\rm in}$ and $\gamma_{\rm out} = 3.5$. Used network size is $N = 10^7$. ○'s denote the estimates for the k algorithm with $r = 0$ and □'s denote those for the ℓ algorithm with $r = 0.5$. The solid curve represents the HMF theory; $\alpha_{\rm HMF} = 1/(\gamma_{\rm in} - 2)$ for $\gamma_{\rm in} < 3$ and $\alpha_{\rm HMF} = 1$ for $\gamma_{\rm in} \geqslant 3$, for both algorithms.

estimates of α from simulations on the networks with various $\gamma_{\rm in}$ and $\gamma_{\rm out} = 3.5$ from both algorithms. As in $A + A \to 0$, the estimates somewhat deviate from the predictions of the HMF theory. However, taking into account the strong finite-size effect, the results agree well with the theory.

Finally, the validity of the quasistatic approximation is examined for the k algorithm with $r = 0$. For this, we measure ρ_k^A, the average density of A particles on the nodes with the same in-degree k. Figure 8(a) shows ρ_k^A at several time steps on

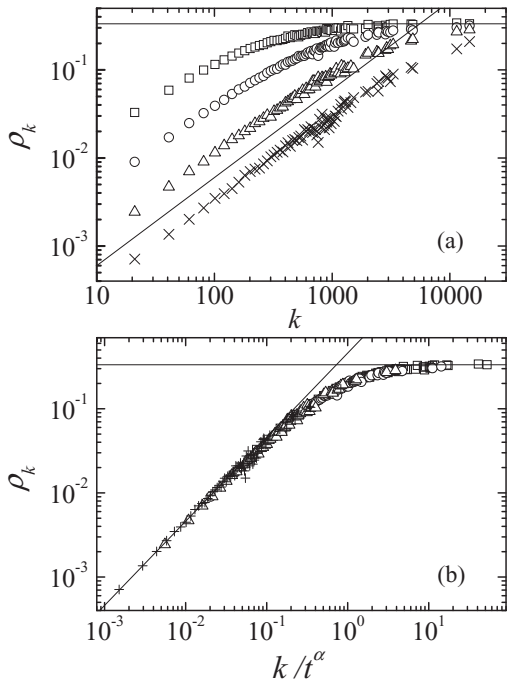

FIG. 8. (a) Plot of $\rho_k(t)$ of $A + B \to 0$ for the k algorithm with $r = 0$ against k at $t = 20\,(\square), 40\,(\circ), 80\,(\triangle)$, and 160 $(\times)$. Used networks are those with $\gamma_{\rm in} = 2.5$, $\gamma_{\rm out} = 3.5$ and $N = 10^7$. (b) Scaling plot of ρ_k against $kt^{-\alpha}$ with $\alpha = 1.88$. In (a) and (b), solid lines represent the theoretical relations $\rho_k \sim k$ for $k \ll k_c$ and $\rho_k = 1/2$ for $k \gg k_c$.

the networks of $(\gamma_{\rm in}, \gamma_{\rm out}) = (2.5, 3.5)$. The plot clearly shows that ρ_k^A linearly increases with k for $k/k_c \ll 1$ and finally saturates to a constant $1/3$ for $k/k_c \gg 1$, as predicted by Eq. (14). The same scaling relation as Eq. (17) is also valid for $\rho_{k\ell}^A$. Figure 8(b) shows that the scaling relation with α obtained from Fig. 6 holds as well. Therefore, we confirm that the quasistatic approximation is also valid for $A + B \to 0$ and thus the HMF theory correctly describes the kinetics of both reactions.

IV. SUMMARY AND DISCUSSION

In summary, we investigate the kinetics of irreversible bimolecular chemical reactions $A + A \to 0$ and $A + B \to 0$ on directed scale-free networks with the in-degree distribution $P_{\rm in}(k) \sim k^{-\gamma_{\rm in}}$ and the out-degree distribution $P_{\rm out}(\ell) \sim \ell^{-\gamma_{\rm out}}$ using the HMF theory and Monte Carlo simulations. Since the in-degree k and the out-degree ℓ of a node are generally correlated in directed networks [23], the correlation between the degrees of a node is controlled by two different algorithms, i.e., the k algorithm of Eq. (6) and the ℓ algorithm of Eq. (9).

From the HMF analysis, the density $\rho_{k\ell}$ of a node with k and ℓ can be written in a simple form as $\rho_{k\ell}(t) \simeq (k/k_c)/(1 + k/k_c)$ for both reactions apart from a prefactor. k_c is the crossover degree defined as $k_c = \langle k \rangle / \rho(t)$. $\rho_{k\ell}$ is a function of only in-degree k, i.e., $\rho_{k\ell} = \rho_k$, and thus independent of the correlation. On undirected scale-fee networks with $P(q) \sim q^{-\gamma}$, the density ρ_q satisfies the same equation [20–22] if the in-degree k of directed networks is replaced by the degree q of undirected networks. The same equations for both directed and undirected networks result from the fact that the inflow of particles into a node is controlled by the in-degree of the node. $\rho_{k\ell}$ linearly increases with k for $k < k_c$ and approaches to a constant for $k > k_c$ as in the undirected networks. The hub nodes with $k > k_c$ maintain a constant particle density in such a way that once the particle on the hub disappears due to the reactions, the particles on the nearest neighbors linked to the hub immediately try to occupy the empty hub.

Furthermore, the equation for $\rho_{k\ell}$ from the HMF theory gives the same type of the rate equation for both reactions as $d\rho/dt = a\rho^2 + b\rho^{\theta-1}$, where θ is $\theta = \gamma_{\rm in}$ for the k algorithm [see Eq. (8)] and $\theta = \gamma_{\rm min}$ for the ℓ algorithm [see Eq. (11)]. For $\theta > 3$, one observes $\rho \sim 1/t$ with $\alpha = 1$. In contrast, for $\theta < 3$, $\rho(t)$ anomalously decays with $\alpha_{\rm HMF} = 1/(\theta - 2)$ due to the strong inhomogeneity of degree distributions. On the undirected networks, $d\rho/dt$ satisfies the same equation with $\theta = \gamma$ [20–22]. Hub nodes with $k > k_c$ maintain a constant density and play as the drains of particles through which particles disappear due to the reactions as in the undirected networks [20]. Thus, $d\rho/dt$ is proportional to the number of the hub nodes, i.e., $d\rho/dt \sim -\int_1^\infty d\ell \int_{k_c}^\infty dk\, P(k,\ell)$, which also gives the $\alpha_{\rm HMF}$ obtained from Eqs. (8) and (11).

Simulations are performed to confirm the predictions of the HMF theory on the quenched directed networks. The estimated α's for both reactions on the networks with various $\gamma_{\rm in}$ are plotted and compared to the HMF theory or $\alpha_{\rm HMF}$ in Figs. 3 and 7. However, a finite maximal in-degree $k_{\rm max}$ of a finite-size network induces the crossover time τ_c above which $\rho(t)$ decays as $\rho(t) \sim t^{-1}$ for any $\gamma_{\rm in}$. For $t < \tau_c$, the kinetics is not affected by the finite size yet, and thus $\rho(t)$ tends to follow the decay

with $\alpha > 1$. The estimates of $\alpha\,(> 1)$ from simulations are smaller than $\alpha_{\rm HMF}$ due to small τ_c for finite N. On the networks with $k_{\rm max} \sim N^{1/(\gamma_{\rm in}-1)}$, τ_c is numerically confirmed to scale with N as $\tau_c \sim N^{1/\mu}$ with $\mu = \alpha_{\rm HMF}(\gamma_{\rm in} - 1)$. Since τ_c slowly increases with N due to large $\mu(> 1)$, it is practically hard to observe the asymptotic HMF behavior on the moderate-size networks. However, the measured α is expected to approach to $\alpha_{\rm HMF}$ in the limit $N \to \infty$ because the measured α is confirmed to increase with N.

Equations (4) and (14) for $\rho_{k\ell}$ are one of the main results of the HMF theory because $\rho_{k\ell}$ gives important physics such as the existence of k_c and the information for the finite-size effect. Hence, in addition to the precise estimation of α and μ, another way to confirm the validity of the HMF theory for both reactions is to examine Eq. (4). $\rho_{k\ell}$ is a function of one scaling variable k/k_c, so it can be simply written as $\rho_{k\ell} = f(k/k_c) = F(kt^{-\alpha})$ [see Eq. (17)]. From the scaling plot of $\rho_{k\ell}$ as in Figs. 5(b) and 8(b), the scaling relation (17) is numerically confirmed and the scaling exponent α is the same as that directly obtained from the data of $\rho(t)$.

All of the simulation results consistently support the predictions of the HMF theory for both reactions on the quenched directed networks. In addition, the HMF theory is exact on annealed networks by definition where links between nodes are rearranged in time [35,36]. Therefore, we conclude that the HMF theory correctly describes the kinetics of both reactions on the directed networks regardless of how quenched the connectivity is in the networks.

ACKNOWLEDGMENTS

This work was supported by National Research Foundation of Korea (NRF) grants funded by the Korean Government (MEST) (Grants No. 2011-0015257 and No. 2012-047246).

[1] N. G. van Kampen, *Stochastic Processes in Physics and Chemistry* (North-Holland, Amsterdam, 1981).
[2] V. Privman, *Nonequilibrium Statistical Mechanics in One Dimension* (Cambridge University Press, Cambridge, UK, 1997).
[3] A. A. Ovchinnikov and Ya. B. Zeldovich, Chem. Phys. **28**, 215 (1978).
[4] D. Toussaint and F. Wilczek, J. Chem. Phys. **78**, 2642 (1983).
[5] B. P. Lee, J. Phys. A **27**, 2633 (1994).
[6] K. Kang and S. Redner, Phys. Rev. Lett. **52**, 955 (1984); Phys. Rev. A **32**, 435 (1985).
[7] B. P. Lee and J. Cardy, J. Stat. Phys. **80**, 971 (1995).
[8] U. C. Täuber, M. Howard, and B. P. Lee, J. Phys. A **38**, R79 (2005).
[9] S. A. Janowsky, Phys. Rev. E **51**, 1858 (1995).
[10] I. Ispolatov, P. L. Krapivsky, and S. Redner, Phys. Rev. E **52**, 2540 (1995).
[11] S. Kwon and Y. Kim, Phys. Rev. E **75**, 021122 (2007).
[12] S. Kwon, S. Y. Yoon, and Y. Kim, Phys. Rev. E **73**, 025102(R) (2006); **74**, 021109 (2006).
[13] S. Kwon and Y. Kim, Phys. Rev. E **79**, 041132 (2009); **82**, 011109 (2010).
[14] S. N. Dorogovtsev and A. V. Goltsev, Rev. Mod. Phys. **80**, 1275 (2008).
[15] R. Albert and A.-L. Barabási, Rev. Mod. Phys. **74**, 47 (2002).
[16] M. E. J. Newman, SIAM Rev. **45**, 167 (2003).
[17] L. K. Gallos and P. Argyrakis, Phys. Rev. Lett. **92**, 138301 (2004).
[18] L. K. Gallos and P. Argyrakis, Phys. Rev. E **72**, 017101 (2005).
[19] L. K. Gallos and P. Argyrakis, Phys. Rev. E **74**, 056107 (2006).
[20] M. Catanzaro, M. Boguñá, and R. Pastor-Satorras, Phys. Rev. E **71**, 056104 (2005).
[21] S. Weber and M. Porto, Phys. Rev. E **74**, 046108 (2006).
[22] S. Kwon, W. Choi, and Y. Kim, Phys. Rev. E **82**, 021108 (2010).
[23] A. Broder, R. Kumar, F. Maghoul, P. Raghavan, S. Rajagopalan, R. Stata, A. Tomkins, and J. Wiener, Comput. Netw. **33**, 309 (2000).
[24] M. E. J. Newman, S. Forrest, and J. Balthrop, Phys. Rev. E **66**, 035101 (2002); Holger Ebel, L.-I. Mielsch, and S. Bornholdt, *ibid.* **66**, 035103 (2002).
[25] A. Grönlund, Phys. Rev. E **70**, 061908 (2004).
[26] P. Bajardi, A. Barrat, F. Natale, L. Savini, and V. Colizza, PLoS ONE **6**, e19869 (2011).
[27] N. Schwartz, R. Cohen, D. ben-Avraham, A.-L. Barabási, and S. Havlin, Phys. Rev. E **66**, 015104 (2002).
[28] S.-G. Han, J. Um, and B. J. Kim, Phys. Rev. E **81**, 057103 (2010), and references therein.
[29] A. D. Sánchez, J. M. López, and M. A. Rodríguez, Phys. Rev. Lett. **88**, 048701 (2002).
[30] J. Wang and Z. Liu, J. Phys. A **42**, 355001 (2009).
[31] H. H. K. Lentz, T. Selhorst, and I. M. Sokolov, Phys. Rev. E **85**, 066111 (2012).
[32] S. Kwon and Y. Kim, Phys. Rev. E **87**, 012813 (2013).
[33] J. D. Noh and H. Park, Phys. Rev. E **79**, 056115 (2009).
[34] M. Catanzaro, M. Boguña, and R. Pastor-Satorras, Phys. Rev. E **71**, 027103 (2005).
[35] R. Pastor-Satorras and A. Vespignani, Phys. Rev. Lett. **86**, 3200 (2001).
[36] C. Castellano and R. Pastor-Satorras, Phys. Rev. Lett. **105**, 218701 (2010); C. T. Butts, Science **325**, 414 (2009).